Macedonian Journal of Chemistry and Chemical Engineering, Vol. **44**, No. 2, pp. 349–366 (2025)

MJCCA9 – 349

ISSN 1857-5552
e-ISSN 1857-5625

Received: September 3, 2025
Accepted: October 9, 2025

DOI: 10.20450/mjcce.2025.3267
Original scientific paper

DUAL ROLE OF LIGNIN IN WATERBORNE POLYMER COMPOSITES: REINFORCEMENT AND STIMULI-TRIGGERED DEGRADATION

Marija Proševa[1], Andrea Petanova[1], Radmila Tomovska[2,3*], Jadranka Blaževska Gilev[1*]

[1]Ss. Cyril and Methodius University in Skopje, Faculty of Technology and Metallurgy, Ruger Bosković 16, 1000 Skopje, N. Macedonia
[2]POLYMAT and Departamento de Química Aplicada Facultad de Ciencias Químicas University of the Basque Country, Joxe Mari Korta Center – Avda. Tolosa, 72 20018, Donostia-San Sebastian, Spain
[3]IKERBASQUE, Basque Foundation for Science, 48011 Bilbao, Spain

jadranka@tmf.ukim.edu.mk; radmila.tomovska@ehu.eus

Improving the sustainability of polymer composites is a pressing priority, particularly in reducing reliance on fossil-derived components and minimising environmental impact during synthesis. Lignin, an abundant and renewable natural polymer, offers significant potential as a bio-based additive due to its aromatic structure and intrinsic functionality. Conventional methods for incorporating lignin into polymer matrices often rely on non-sustainable, solvent-based routes, leading to poor dispersion and aggregate formation due to lignin's incompatibility with polymers. This study presents a more sustainable approach using waterborne, in situ semicontinuous miniemulsion polymerisation to integrate lignin (0.5–1 wt%) into (meth)acrylic matrices. The resulting composite films, formed via water evaporation, exhibited enhanced UV and visible light absorption, improved mechanical strength, particularly at 1 wt% lignin, and increased thermal stability even at low loadings. Despite lignin's hydrophilicity, the composites demonstrated reduced water permeability. Ultraviolet degradation studies showed that lignin's chromophoric groups generate free radicals under UV exposure, triggering controlled photodegradation of both lignin and polymer phases. This controlled breakdown, combined with the composite's enhanced structural integrity, highlights lignin's dual function: reinforcing the material under standard conditions while enabling degradation under specific environmental stimuli.

Keywords: lignin; sustainable materials; polymer composites; UV-triggered degradation

ДВОЈНА УЛОГА НА ЛИГНИНОТ ВО ВОДОДИСПЕРЗИБИЛНИ ПОЛИМЕРНИ КОМПОЗИТИ: ЗАЈАКНУВАЊЕ И ДЕГРАДАЦИЈА ПРЕДИЗВИКАНА ОД НАДВОРЕШНИ ВЛИЈАНИЈА

Подобрувањето на одржливоста на полимерните композити е важен приоритет, посебно во намалувањето на зависноста од ресурси добиени од фосилни горива и намалувањето на влијанието врз животната средина за време на синтезата. Лигнинот, обновлив природен полимер кој го има во изобилство, поседува голем потенцијал како биобазиран адитив поради неговата ароматична структура и висока функционалност. Конвенционалните методи за инкорпорирање на лигнин во полимерни матрици честопати се базираат на неодржливи методи базирани на растворувачи, што доведува до слаба дисперзија и формирање на агрегати поради некомпатибилноста на лигнинот со полимерите. Ова истражување, со користење на вододисперзибилна, *in situ* полуконтинуирана миниемулзиска полимеризација демонстрира поодржлив пристап кон инкорпорирање на лигнин (0,5 – 1 масени %) во (мет)акрилни матрици. Добиените композитни филмови, формирани преку испарување на вода, поседуваа подобрена апсорпција на УВ и видлива светлина, подобрена механичка цврстина, особено при 1 масен % лигнин, и зголемена термичка стабилност дури и при ниски концентрации. И покрај хидрофилноста на лигнинот, композитите покажаа намалена дифузија на вода. Испитувањето поврзано со деградацијата предизвикана од ултравиолетова

светлина укажа на тоа дека хромофорните групи на лигнинот генерираат слободни радикали при изложеност на УВ–зрачење, предизвикувајќи контролирана фотодеградација и на лигнинот, но и на полимерната фаза. Ова контролирано распаѓање, во комбинација со подобрениот структурен интегритет на композитот, ја истакнува двојната функција на лигнинот: зајакнување на материјалот под стандардни услови, а воедно овозможува деградација под специфични влијанија од животната средина.

Клучни зборови: лигнин; одржливи материјали; полимерни композити; УВ-деградација

1. INTRODUCTION

Modern life is deeply dependent on the use of polymers and polymer-based composites, largely due to their low production costs and wide-ranging functional properties. However, most of these materials are still derived from non-renewable petroleum resources.[1,2] This dependency not only accelerates the depletion of finite natural reserves but also exacerbates environmental challenges, negatively impacting human health and overall quality of life.

A more sustainable strategy for producing polymers and their composites involves the gradual replacement of petroleum-based monomers and synthetic fillers, typically obtained via chemical synthesis or the intensive processing of raw materials such as metal oxides or organic substances,[3] with renewable alternatives. These renewable feedstocks are often by-products of other industrial processes and offer several key advantages, including lower extraction costs, recyclability, and biodegradability.[1,2,4]

Lignin is one of the primary components of lignocellulosic biomass[5] and is commonly generated as a by-product in various industries, including pulp and paper, tobacco, and agriculture. According to Fabbri et al., global lignin production is approximately 100 million tonnes annually.[6] In 2023, the global lignin market was valued at $1.08 billion USD and is projected to grow at a compound annual growth rate (CAGR) of 4.5 % between 2024 and 2030.[7] Despite this substantial production, a large portion of lignin is either discarded to landfills or used as a low-value energy source.[2] However, when lignin derived from waste streams is repurposed, it supports sustainability by reducing waste and enabling the development of value-added products. This approach not only reduces reliance on fossil resources but also contributes to lower greenhouse gas emissions and advances the principles of a circular economy.

Lignin is a natural polymer characterised by a complex aromatic structure that varies depending on its source.[8,9] Its polymeric framework is primarily composed of three monolignols: sinapyl alcohol, coniferyl alcohol, and p-coumaryl alcohol,[6,9,10]which are interconnected through arylglycerol ether bonds. The relative abundance of these monolignols depends on the origin of the raw material from which the lignin is extracted.

Lignin's complex chemical structure endows it with a wide range of properties, making it highly researched for diverse applications.[4,11] For example, its antioxidant properties make lignin an ideal filler for synthesising composites with enhanced oxidative stability.[11–19] Additionally, its high thermal stability renders it a suitable filler for composites with reduced flammability.[20–25] Lignin's antimicrobial activity further broadens its potential in the field of biomaterials.[26–28] Moreover, its intricate structure and the presence of functional groups, including as hydroxyl, carbonyl, and methoxy groups, make lignin an effective adsorbent for both organic and inorganic water pollutants.[29–33]

Additionally, the incorporation of lignin into composite films significantly accelerates the degradation of polymer/lignin composites, particularly under UV exposure and humid conditions, due to its ability to absorb UV radiation through chromophoric groups.[34–36] This UV absorption leads to the generation of reactive species, including free radicals and p-quinone structures, which initiate photodegradation in both the lignin and polymer phases. These reactive intermediates promote chain scission within the polymer matrix, resulting in the breakdown of long polymer chains and the formation of new functional groups such as carbonyl and vinyl groups. Moreover, lignin's chemical structure, inherent hydrophilicity, and physical interactions with the polymer matrix enhance moisture absorption. This increased moisture uptake accelerates degradation by promoting hydrolysis and elevating the composite's chemical reactivity.[2,35,36] Lignin incorporation also alters the crystallinity of the composite and disrupts the polymer network, making the material more susceptible to enzymatic degradation and further environmental deterioration.[36] Therefore, the presence of lignin in these composites forms the foundation for developing various pathways for triggered degradation and sustainable recycling.

Lignin-based polymer composites are typically prepared through melt mixing or solution mixing.[2,12–14,17,19,22,26–28,37] However, these conventional methods present several notable limitations. Melt mixing, for example, requires high processing temperatures ranging from 160 to 210 °C,[6,8,14,15,23] while solution mixing often involves the use of toxic organic solvents such as tetrahydrofuran,[14] chloroform,[16] dioxane,[27] and dimethyl sulfoxide.[28] Another major drawback of these methods is the frequent inability to achieve a uniform dispersion of lignin within the polymer matrix.[38] This challenge is largely due to lignin's inherent tendency to agglomerate, driven by its complex chemical structure.[2] Poor dispersion can significantly compromise the performance and properties of the final composite material.

In situ polymerisation offers a promising alternative to overcome filler dispersion challenges. This approach involves integrating the filler between polymer chains during the polymerisation process, which prevents agglomeration and enhances compatibility with the polymer matrix.[39] However, conventional in situ methods remain cumbersome, often requiring prior chemical modification of lignin[24,25,40] and involving lengthy, multi-step procedures.[33] To bypass these limitations, aqueous dispersed polymerisations have been explored, where emulsifiers stabilise lignin in water prior to polymerisation, promoting its dispersion in the polymer matrix. Miniemulsion polymerisation offers enhanced control over particle size, polymer properties, and morphology, making it a preferred method for synthesising polymers and polymer-based composites.[41,42] Only two studies to date have attempted this strategy with lignin using miniemulsion and emulsion polymerisations.[43,44] Both reported procedures suffered from critical drawbacks, including multi-step initiator addition schemes, discontinuous lignin, and extended reaction times (up to 6 h). Such discontinuous processes not only complicate operation but also undermine reproducibility, while conversions remained highly dependent on lignin type and concentration.[43,44] At 0.7 wt% kraft lignin, conversion remained low (~20%), while 0.7 wt% lignosulfonate achieved ~70%.[43] In another study, conversion reached ~67% with 1 wt% kraft lignin (3 h, initiator every 20 min), but dropped to ~53–55% at 2 wt% depending on polymerisation time (3 and 6 h).[44] Both methods relied on discontinuous reactant additions, limiting reproducibility.

The present study introduced an optimised and more robust approach to overcome these limitations. (Meth)acrylic monomers with film-forming potential were polymerised via miniemulsion in the presence of surfactant-stabilised lignin, but with a key adjustment: lignin was continuously introduced through controlled dropwise feeding during the polymerisation process. This simple, effective reaction engineering strategy fundamentally improved continuity and reproducibility by avoiding batch-wise lignin or initiator additions. Moreover, by maintaining lignin at low instantaneous concentrations, its radical scavenging activity was mitigated, enabling high monomer conversions even at 0.5 – 1 wt% lignin loading—levels where previous methods showed dramatic conversion losses. Beyond improving process efficiency and scalability, this strategy produced stable, film-forming aqueous dispersions with well-dispersed lignin, while simultaneously imparting tuneable functional properties, including UV-triggered recyclability. In doing so, the study established a versatile and scalable synthesis route that directly addressed the shortcomings of earlier approaches and advanced the design of sustainable lignin–polymer nanocomposites. The simplicity of the continuous lignin addition, combined with waterborne dispersions and low lignin loadings, suggested that this approach could be readily adapted to industrial-scale production, providing a sustainable route for producing functional polymer composites for applications such as coatings, packaging, and films.

2. EXPERIMENTAL SECTION

2.1. *Materials*

An aqueous dispersion of lignin was prepared using kraft lignin (hereafter abbreviated as L) and sodium dodecyl sulphate (SDS, 98 % purity) as the surfactant, both obtained from Sigma-Aldrich. St. Louis, MO, USA. The neat polymer and the composites were synthesized using methyl methacrylate (MMA, 99 % purity), butyl acrylate (BA, 99 % purity), and acrylamide (Aam, 99 % purity), all purchased from Sigma-Aldrich, St. Louis, MO, USA. Stearyl acrylate (SA, 97 % purity) from Sigma-Aldrich, St. Louis, MO, USA served as the costabiliser. Dowfax 2A1 solution (45 %, alkyldiphenyloxidedisulfonate) from Dow Chemical Company, Midland, MI, USA was used as an additional surfactant. Azobisisobutyronitrile (AIBN, 98 % purity) from Sigma-Aldrich, St. Louis, MO, USA acted as the initiator. Deionised water, BIOBASE Deionized Water Purifier (13~16 MΩ-cm) was utilised throughout the experiments.

2.2. *Methods*

2.2.1. *Aqueous dispersion of lignin*

An appropriate amount of SDS (L:SDS weight ratio of 1:1) was dissolved in deionised water and stirred for 30 minutes. Lignin was then added at concentrations of 0.5 wt% and 1 wt% relative to the monomer content. The resulting dispersion was homogenised using a tip sonicator (UP200Ht, Hielscher Ultrasonics GmbH, Germany) in an ice bath under the following conditions: 70 % amplitude, 50 % duty cycle, 10 minutes of effective sonication time, and continuous agitation at 200 rpm.

2.2.2. *In situ miniemulsion polymerisation*

The monomers MMA, BA, and AAm were combined in a weight ratio of 49.5 : 49.5 : 1, together with the stabiliser SA, (6 wt% based on monomers) and the initiator AIBN (0.5 wt% based on monomers). The mixture was stirred until the AAm, SA, and AIBN were fully dissolved. Dowfax surfactant (2 wt% based on monomers), pre-dissolved in water, was then added to the beaker. The monomer content was adjusted to obtain a total solids content of 20%. The mixture was homogenised using a tip sonicator under the following conditions: 70 % amplitude, 50 % duty cycle, 15 minutes of effective sonication time, and continuous agitation at 200 rpm. The beaker was placed in an ice bath during homogenisation to maintain low temperature. The prepared miniemulsion was transferred to a 250 ml glass reactor equipped with a water bath for heating. The miniemulsion was stirred continuously, and nitrogen was bubbled through the system for the first 2 minutes to remove dissolved oxygen. The polymerisation reaction was initiated once the miniemulsion reached 70 °C. Lignin was incorporated using a feeding approach, where an aqueous lignin dispersion was added dropwise into the miniemulsion. Feeding began 10 minutes after the miniemulsion reached 70 °C and continued at a flow rate of approximately 0.875 g/min for 40 minutes. After lignin addition was complete, polymerisation proceeded for a further 40 minutes. Scheme 1 illustrates the in situ miniemulsion synthesis of lignin/polymer composites.

A neat (lignin-free) polymer was prepared under identical conditions, with the total water content introduced directly into the miniemulsion at the start. Table 1 summarises the formulations used for synthesising each sample.

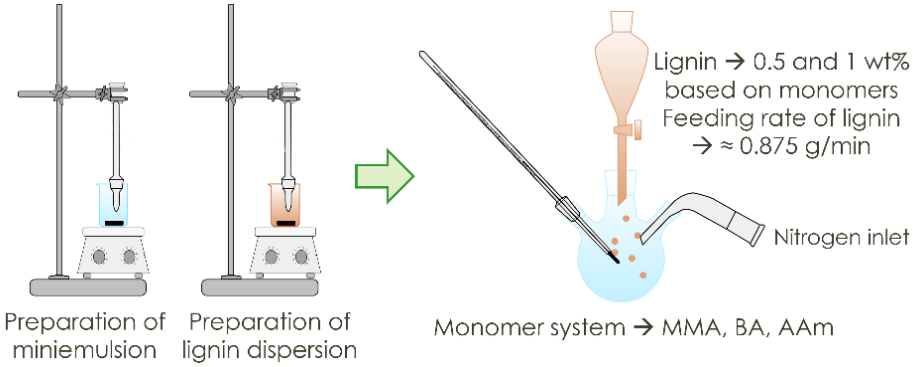

Scheme 1. In situ miniemulsion synthesis of lignin/polymer composites

T a b l e 1

Formulations for the synthesis of the samples

Sample	Miniemulsion (g)						
	MMA	BA	AAm	SA	AIBN	Dowfax	Water
P(MMA/BA/AAm)	9.5	9.5	1	1.2	0.1	0.4	80
0.5 wt% L/P(MMA/BA/AAm)	9.5	9.5	1	1.2	0.1	0.4	50
1wt% L/P(MMA/BA/AAm)	9.5	9.5	1	1.2	0.1	0.4	50

Sample	Feeding batch (g)		
	Lignin	SDS	Water
P(MMA/BA/AAm)	/	/	/
0.5 wt% L/P(MMA/BA/AAm)	0.1	0.1	30
1wt% L/P(MMA/BA/AAm)	0.2	0.2	30

Monomer conversion was monitored gravimetrically by weighing the neat polymer and composite dispersions before and after drying at room temperature for 48 h. The dispersions were cast into silicone moulds and dried under ambient conditions (23°C and 55 % humidity) over five days. Figure 1 illustrates the free-standing films of the neat polymer and the composites.

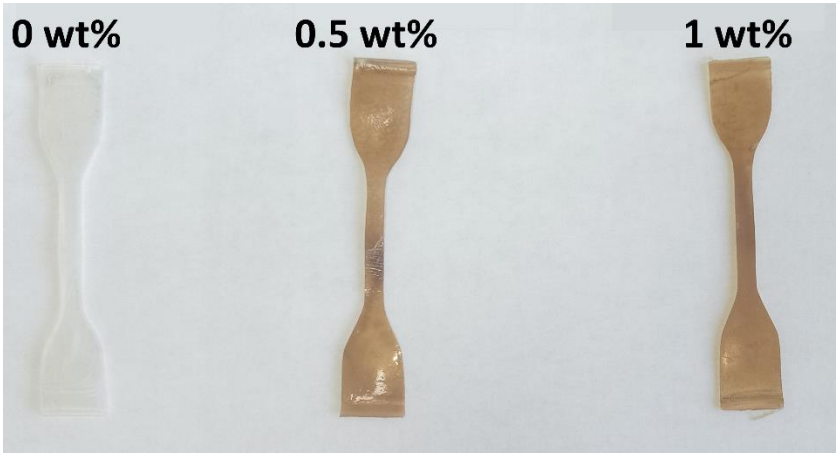

Fig. 1. Free-standing films of the neat polymer (0 wt%) and composites containing 0.5wt% and 1wt% lignin

2.3. *Characterisation*

The successful incorporation of lignin into the polymer matrix was verified by obtaining infrared spectra of the solid composite films with Fourier transform infrared spectroscopy (FTIR) equipped with attenuated total reflection (ATR) (PerkinElmer Spectrum 100, Shelton, CT, USA), operating over 20 scans. The scanning range extended from 4000 to 650 cm^{-1}. The spectra were analysed using OMNIC software (Thermo Fisher Scientific, Waltham, MA, USA).

To assess the influence of lignin on absorption in the ultraviolet and visible regions, the composites were examined using ultraviolet–visible spectroscopy (UV–Vis) (UV-Mini 1240 Shimadzu, Kyoto, Japan). The spectra were processed using UVProbe 2.42 software.

To eliminate the effect of sample thickness on UV and visible light absorption, the absorption coefficient, α [cm^{-1}], was calculated using Equation 1:[45]

$$\alpha = 2.303 \times \frac{A}{d} \quad (1)$$

where A represents absorbance and d denotes the sample thickness. The average thickness of samples, based on three measurements, is reported in Table 2.

The composite's ability to absorb UV and visible light was quantified via band gap energy using Tauc plots, which relate the absorption coefficient to the optical band gap (E_g), as shown in Equation 2:

$$\alpha h\nu = B\left(h\nu - E_g\right)^m \quad (2)$$

where h denotes Planck's constant (6.62607015 × 10^{-34} m^2 kg/s), ν is the frequency, B (proportionality constant) is the slope of the linear portion of the Tauc plot, constant, and m is a parameter defining electron transition. For direct allowed transitions (E_{da}), m = 2; for indirect allowed transitions (E_{ia}), m = ½.[45]

T a b l e 2

Thickness of the samples

Sample	Thickness (mm)
P(MMA/BA/AAm)	0.90
0.5 wt% L/P(MMA/BA/AAm)	0.54
1wt% L/P(MMA/BA/AAm)	0.68

The morphology of the composites was analysed using scanning electron microscopy (SEM). A Quanta 250 e – SEM (Philips Tecna, FEI, Eindhoven, Netherlands) instrument was employed for this purpose. Cross-sectional images were obtained from films fractured in liquid nitrogen and then sputter-coated with gold to improve conductivity and minimising charging artifacts.

The contact angle of the samples with distilled water, together with surface energy, was de-

termined using See System E instrument (Advex Instruments, Brno, Czech Republic) via the sessile drop method, analysed with See System E software. Images were captured using a Colour 2Mpix (1600×1200) UVC camera with a high-resolution glass objective lens. Surface energy was calculated using the Owens–Wendt model[46] with distilled water and ethylene glycol as probe liquids. The reported values for both contact angle and surface energy represented the average of fifteen individual measurements.

The thermal stability of the samples was assessed using thermogravimetric analysis (TGA) (TA Instruments Q500, New Castle, DE, USA). The test conditions consisted of heating the sample from 40°C to 800°C at a rate of 10 °C/min. The obtained results were processed using TA Universal Analysis software. Temperatures corresponding to 1 %, 10 %, and 50 % mass loss, as well as the percentage of mass loss at the maximum degradation temperature, were recorded. The first derivative of the weight-loss curve (derivative thermogravimetry- DTG) was calculated with OriginPro 2018 (64-bit) software, (Version [SR1 b9.5.1.195] OriginLab Corporation, Northampton, MA, USA) for detailed thermal analysis.

To examine the influence of lignin on mechanical properties, the composites and neat polymer underwent elongation testing using a Universal AutoGraph testing instrument (SHIMADZU 25T type AGX, Japan). The distance between the instrument holders was set at 50 mm and the test speed was maintained at 10 mm/min. Prior to testing, the samples were cut into a standardised dog-bone shape (Fig.1) using a hydraulic press, and their thickness was measured before testing. Mechanical parameters such as Young's modulus, yield strength, tensile strength, and maximum strain at break were calculated using TrapeziumX software. Young's modulus was determined within a stress range of 0.01 – 0.1 MPa, and yield strength was defined at 0.2 % strain. Sample toughness was estimated by integrating the stress-strain curve area using OriginPro 2018 (64-bit) software (Version [SR1 b9.5.1.195] OriginLab Corporation, Northampton, MA, USA). All reported values represented the average of three independent measurements.

To assess the effect of lignin on UV stability, the polymer and composites were aged under 366 nm UV radiation at ambient conditions (25°C and 55 % relative humidity) for 364 hours. For this purpose, a UV lamp hand device manufactured by P-LAB (Prague, Czech Republic) was employed. The device utilizes an internal UV discharge lamp operating at its long-wave UV-A peak of 366 nm. The lamp was operated to deliver an irradiation power of 550 mW/cm^2 on the sample surface, measured at a distance of 15 cm. Photodegradation progress was monitored by analysing the samples with the FTIR-ATR spectrometer setup. With OMNIC software, the areas of the spectral bands related to the hydroxyl (3700 – 3060 cm^{-1}) and ether functional group (1333 – 1075 cm^{-1}) were quantified, and the peak height of the characteristic carbonyl band (1730 cm^{-1}) was measured. The experiments were performed in triplicate.

Water uptake was assessed by submerging five samples of the neat polymer and composites in distilled water for 336 hours at room temperature. Before immersion, sample mass was recorded (m_1), and after immersion, the samples were removed and weighed again (m_t). Water uptake was calculated using Equation 3, and the reported values were the mean of five measurements.

$$M_t(\%) = \frac{m_t - m_1}{m_1} \times 100 \qquad (3)$$

3. RESULTS AND DISCUSSION

Waterborne lignin/polymer composites were prepared via in situ miniemulsion polymerisation, incorporating lignin at concentrations of 0.5 wt% and 1 wt% relative to the polymer. The monomer system comprised MMA and BA in a 1:1 weight ratio, producing aqueous polymer dispersion with film-forming ability at room temperature, attributed to the glass transition temperature T_g of approximately 17 °C.[47] Additionally, AAm was added at 1 wt% to functionalise the polymer and improve compatibility with lignin, facilitating hydrogen bond formation between the amide group and lignin hydroxyl groups. Monomer conversion was measured gravimetrically. The neat polymer reached a conversion rate of 91 %, while the composites containing 0.5 wt% and 1 wt% lignin reached 73 % and 72 %, respectively. The lower conversion rates observed in the composites were attributed to lignin's inherent antioxidative properties.[43] To mitigate this effect during in situ polymerisation, the lignin aqueous dispersion stabilised with SDS was fed into the reactor in a controlled manner to maintain a low concentration. Despite this controlled addition of kraft lignin during polymerisation, its moderate radical scavenging activity continued to interfere with the reaction by capturing free radicals generated by the initiator, reducing monomer conversion. Nevertheless, the monomer conversions achieved in this study were significantly higher than those reported for similar in situ processes incorporating kraft lignin

into a poly(methyl metacrylate) (PMMA) matrix. For instance, in a recent study utilising 0.7 wt% kraft lignin, the monomer conversion was only 10 % –25 %.[43] These results highlighted that strategic reaction engineering during polymerisation served as an effective approach to overcome the challenge of low monomer conversion in lignin-based systems.

After polymerisation, the neat polymer dispersion was milky white, while the composite dispersions showed a light to dark brownish hue. The composite dispersions remained stable for several hours before lignin precipitation occurred. Composite films were cast from these dispersions under standard atmospheric conditions by water evaporation. Homogenous films were obtained in all cases: completely transparent for the neat polymer and light brown for lignin composites (Fig.1). The loss of transparency was likely due to the presence of the lignin phase within the polymer matrix, which induced light scattering.

To confirm lignin incorporation within the polymer matrix, FTIR analysis was conducted. Figure2 shows the FTIR spectra of pristine lignin, the neat polymer (0 wt%), and the composites (0.5 wt% and 1 wt%).

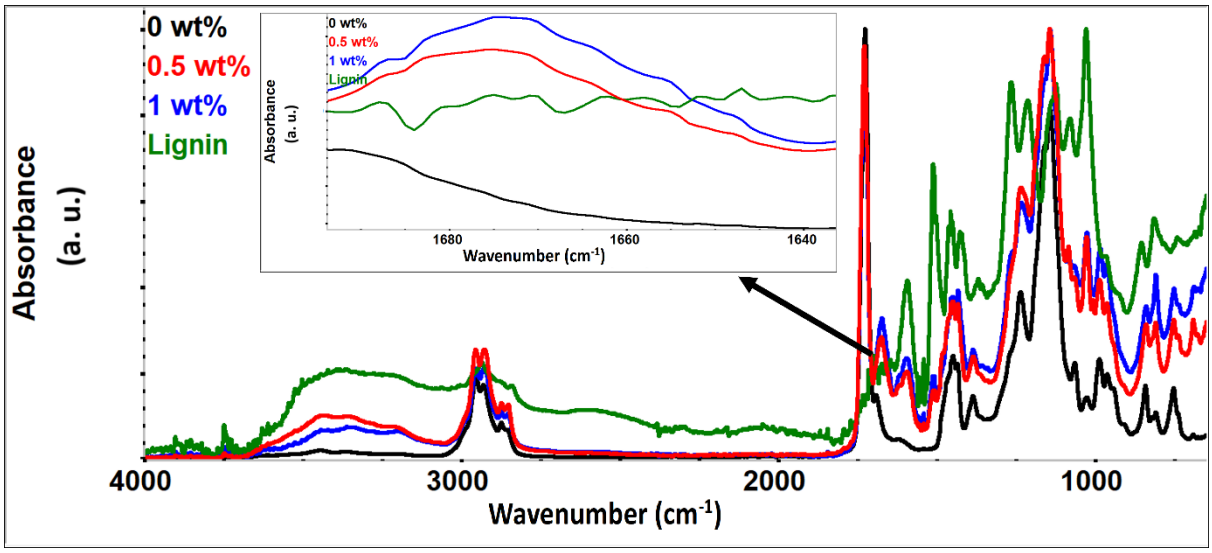

Fig. 2. FTIR-ATR spectra of the neat polymer, lignin, and the composites containing 0.5 wt% and 1 wt% lignin

The lignin spectrum displayed characteristic bands corresponding to the hydroxyl group (OH, 3700–3100 cm^{-1}), a broad band around 1710 cm^{-1} overlapping with bands in the 1600–1400 cm^{-1} range, associated with carbonyl groups and skeletal vibrations of the aromatic ring, respectively, and the ether group (C–O–C, 1300–1000 cm^{-1}). In the neat polymer spectrum, distinct bands for the carbonyl group (C=O, 1730 cm^{-1}) and the ether group (1160 cm^{-1}) were observed. The composite spectra exhibited characteristic bands for the hydroxyl group (3700–3100 cm^{-1}) and aromatic skeletal vibrations (1600–1400 cm^{-1}). Additionally, a notable band appeared at approximately 1675 cm^{-1} (Fig.2, embedded), attributed to the imide group, suggesting a possible reaction between the polymer's amide group and lignin carbonyl groups. The presence of lignin-specific bands, along with the formation of a new characteristic band in the composite spectra, confirmed the successful incorporation of lignin into the polymer matrix.

The optical properties of the composites were influenced by the presence of lignin. To investigate this, UV-Vis spectra were obtained using a UV/Vis spectrophotometer. The UV-Vis spectra and absorption coefficients (α), together with the direct and indirect transitions of the neat polymer and the composites are presented in Figure3. Table 3 summarises the values of the direct and indirect transitions of the neat polymer and the composites.

The phenolic structure of lignin allowed strong UV absorption in the 280–325 nm range, whereas the neat polymer absorbed almost nothing in the visible region. In the composites, the absorption maximum shifted to higher wavelengths compared to the polymer, owing to the conjugated phenolic structure integrated into the polymer matrix. Furthermore, the unsaturated functional groups in lignin significantly enhanced the absorption of visible light compared to the neat polymer. The UV-visible light absorbed by lignin triggered light-

catalysed photo-reactions, leading to the formation of quinones and other chromophoric groups, which in turn absorbed even more UV light. This property made lignin an efficient UV blocker, and its effectiveness was enhanced when exposed to light.[10] To account for potential variations in film thickness that might have influenced the UV absorption measurements, absorption coefficients were determined (Fig.3b). These calculations confirmed that the composites absorbed more UV-visible light, with this effect being more pronounced in the sample with higher lignin content.

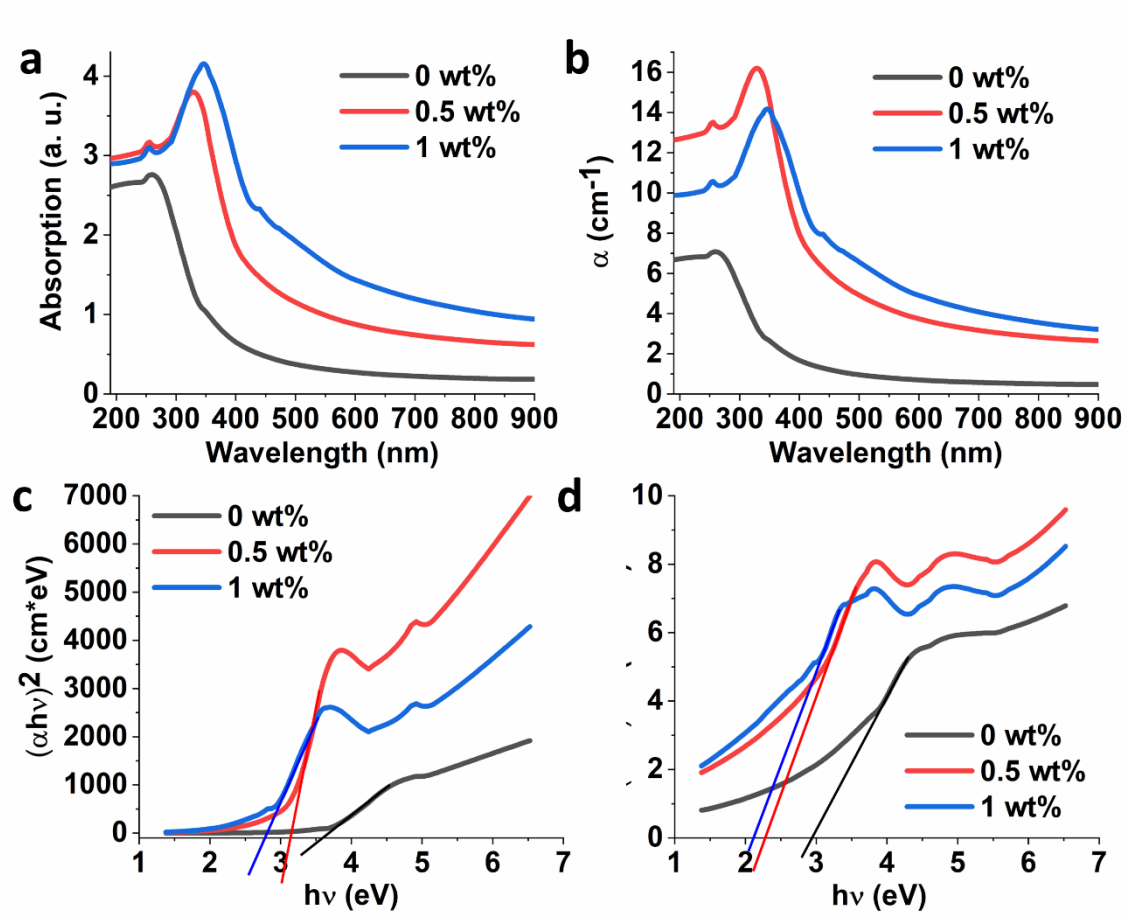

Fig. 3. (a) UV-Vis spectra, (b) absorption coefficients (α), (c) direct allowed transitions (E_{da}), and (d) indirect allowed transitions (E_{ia}) of the neat polymer and the composites films

T a b l e 3

Values of direct and indirect transitions of the neat polymer and the composites

Sample	E_{da} (eV)	E_{ia} (eV)
P(MMA/BA/AAm)	3.61	2.95
0.5 wt% L/P(MMA/BA/AAm)	3.15	2.27
1 wt% L/P(MMA/BA/AAm)	2.78	2.13

The optical band gap energy was calculated from the intercept of the extrapolated linear region by extending the steepest portion of the curve to the abscissa. The band gap corresponded to the point where this line intersected the axis. As shown in Table 3, E_{da} and E_{ia} decreased with lignin incorporation into the polymer matrix, suggesting a reduced bandgap between the valence and conduction bands. For the composite with 1 wt%, this reduction was approximately 0.8-fold. The band gap energy was significant for materials that were strong UV-Vis absorbers, since it determined the minimum energy, and therefore the minimum wavelength, of light that a material could absorb. This property was essential for applica-

tions requiring specific light absorption.[48] The results for the optical band gap confirmed the observations from the UV-Vis spectra and absorption coefficients; i.e. lignin incorporation led to enhanced absorption of visible light.

The morphology of the samples was examined using SEM. Figure 4 shows cross-sections of the neat polymer films (Figs. 4a–4c), the composite film with 0.5 wt% lignin (Figs. 4d–4f), and the composite film with 1 wt% lignin (Figs. 4g–4i) at different magnifications.

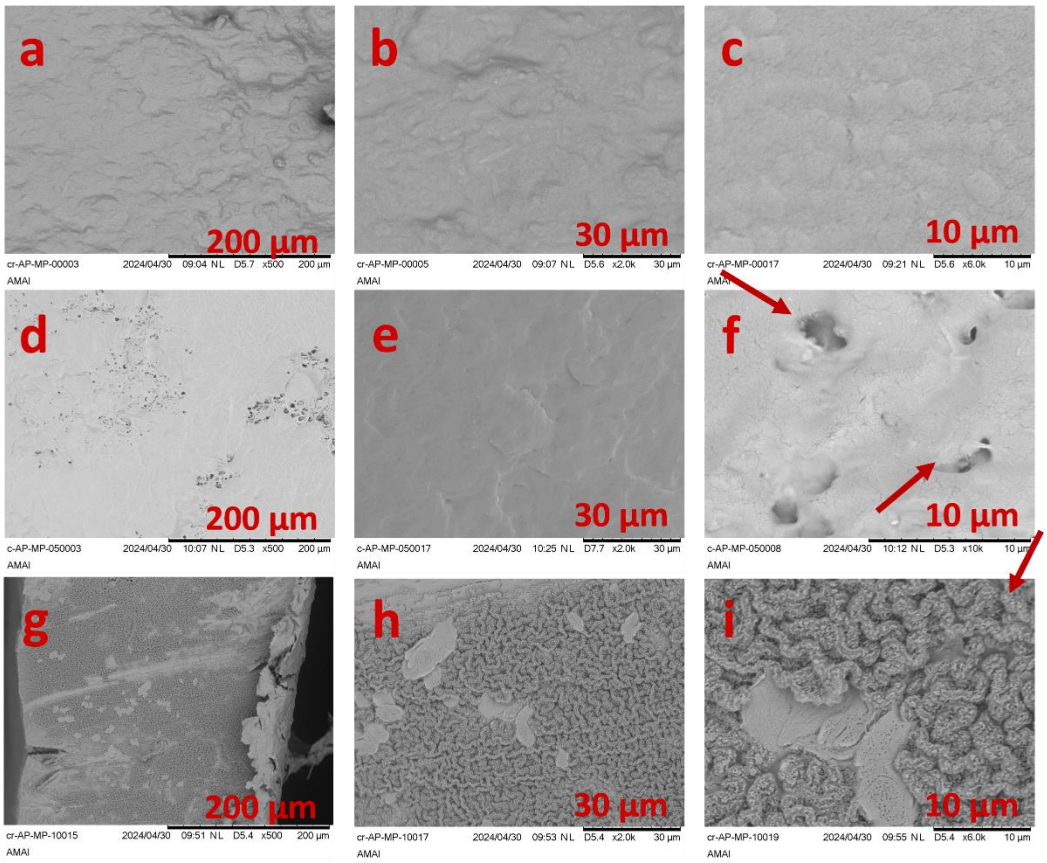

Fig. 4. SEM micrographs showing cross-sections of the neat polymer film (a–c), the composite film with 0.5 wt% lignin (d–f), and the composite film with 1 wt% lignin (g–i) at different magnifications. Arrows indicate pores and surface features relevant to the analysis

The polymer exhibited a relatively smooth cross-section compared to the composites. As the lignin concentration increased, the cross-sectional surface of the composites became noticeably rougher. This effect was particularly pronounced in the composite containing 1 wt% lignin, where distinct "wavy" cross-sectional structures were evident (Figs. 4h and 4i). Pores were observed in the composites, especially in the sample with 0.5 wt% lignin (Figs. 4d–4f). The presence of pores may have originated from drying stresses or particle coalescence effects, but since all samples were dried under identical conditions, it was assumed that these pores likely formed due to phase separation between neat polymer, lignin, and polymer–lignin phases, indicating the presence of these three phases in the system. As the lignin concentration increased from 0.5 to 1 wt%, the size and number of pores decreased. This reduction was likely due to the increased presence of the polymer/lignin phase, which acted as a compatibiliser between neat polymer and lignin; there were many literature reports in which lignin was used as a compatibiliser in different composites systems.[49–51]

Hydrophilicity and water sensitivity of the films were assessed by measuring contact angles and surface energy using the sessile-drop method with distilled water and ethylene glycol. Table 4 summarises the contact angle values and total surface energy, along with the non-polar (γ^{LW}) and polar (γ^{AB}) components of surface energy for both the neat polymer and composite films. The films were examined both before and after rinsing with distilled water to evaluate potential surfactant migration to the sample surfaces.

Table 4

Contact angle, total surface energy, and non-polar (γ^{LW}) and polar (γ^{AB}) components of surface energy of the neat polymer and the composite films, measured before (B) and after (A)rinsing with water

Sample	Contact angle (°)		Total surface energy (mJ/m²)		γ^{LW} (mJ/m²)		γ^{AB} (mJ/m²)	
	B	A	B	A	B	A	B	A
P(MMA/BA/AAm)	85 ± 6	83 ± 9	22	45	7	43	15	2
0.5 wt% L/P(MMA/BA/AAm)	53 ± 7	75 ± 7	50	38	6	30	44	8
1 wt% L/P(MMA/BA/AAm)	47 ± 7	79 ± 7	54	43	7	39	47	4

The contact angle of the films before rinsing decreased with lignin addition compared to the neat polymer film, indicating enhanced hydrophilicity of the composites. This effect was attributed to the hydrophilic functional groups present in the lignin structure, which increased the polarity of the composite surface and elevated the polar component of the surface energy (γ^{AB}). Despite this, the total surface energy of the composites decreased relative to the neat polymer, likely due to disruption of intermolecular interactions within the polymer matrix caused by lignin incorporation. It should be noted, however, that these results were undoubtedly influenced by the presence of surfactant in the waterborne systems, which tended to migrate toward the film surface during formation and further enhanced hydrophilicity.[52]To verify whether this phenomenon had occurred in the present films, the samples were rinsed with water and dried; afterwards their contact angles were measured. Significant changes in contact angle and surface energy were noted after rinsing, particularly in the composite films, which became more hydrophobic. These changes suggest that while the surfactant molecules remained trapped within the neat polymer matrix, they migrated more effectively to the surface in the composites. The likely reason for this migration was the distribution of hydrophilic lignin throughout the film, creating hydrophilic pathways for surfactant movement. Nevertheless, this result revealed that the composite films exhibit a slightly hydrophobic nature. The thermal stability and degradation of the composites was assessed by thermogravimetric analysis (TGA) at a heating rate of 10 °C/min; the samples were heated from 40 °C to 800 °C. Table 5 presents the temperatures corresponding to 1 % mass loss, 10 % mass loss, 50 % mass loss, the maximum degradation temperature, the mass loss at the maximum degradation temperature, and the residue remaining at 750 °C.

Table 5

Temperatures corresponding to 1% mass loss, 10% mass loss, 50% mass loss, maximum degradation temperature, mass loss at maximum degradation temperature, and residue at 750 °C

Sample	$T_{1\%}$ (°C)	$T_{50\%}$ (°C)	T_{max} (°C)	Mass loss at T_{max} (%)	Residue at 750 °C (%)
P(MMA/BA/AAm)	248.10	400.6	400.62	49.66	0.17
0.5wt% L/P(MMA/BA/AAm)	186.48	406.54	410.26	54.47	2.37
1wt% L/P(MMA/BA/AAm)	195.35	409.55	411.29	65.88	1.83

In Figure 5, the TGA curves and the first derivative curve of the mass loss curve (DTG) are shown. According to the TGA results, the 1% mass loss in the composites occurred at a significantly lower temperature compared to the neat polymer. The mass loss in composites at lower temperature was due to the presence of lignin. Namely, lignin contained hydroxyl and methoxy functional groups in its structure that were eliminated at lower temperatures, hence the mass loss at lower temperatures in the composites. The 50% mass loss occurred at a higher temperature in the composites compared to the polymer. According to the DTG curves, the degradation of the samples occurred in one step, and the maximum peak in the composites was shifted by 10 °C and 11 °C for the 0.5 wt% and 1 wt% composites, respectively, compared to the neat polymer. The residual mass at 750 °C was

significantly higher in the composites compared to the polymer (by more than ten times). These results indicated that the incorporation of lignin into the polymer matrix, even at low concentrations of 0.5 wt% and 1 wt%, had a positive effect on the thermal stability of the polymer. The improved thermal stability observed in the composites originated from the structure of lignin, in which polar and aliphatic groups were present in its network. Because lignin contained various aromatic functional groups with different thermal stabilities, its decomposition occurred over a broad temperature range. Additionally, its high carbon content promoted significant char formation in an inert atmosphere, which helped reduce the heat-release rate of the polymeric materials during degradation steps.[53] As a result, the presence of lignin in the polymer matrix enhanced the thermal stability of the polymer composites. In addition to the intrinsic thermal properties of lignin, the enhanced thermal stability observed here may have also arisen from improved interfacial interactions between lignin and the polymer matrix. For comparison, Assumpção et al. prepared PMMA/lignosulfonate composites (0.7 wt% lignosulfonate) via in situ miniemulsion polymerisation and achieved satisfactory conversion; however, they reported that lignin addition did not lead to improved thermal stability.[43] Messmer et al., in their study, were not able to confirm whether the introduction of kraft lignin had any significant influence on the thermal behaviour of the polymer.[44]

The mechanical properties of the prepared samples were assessed using tensile testing. Table 6 presents the average values (based on three measurements) for yield strength, modulus of elasticity, tensile strength, strain at break, and toughness.

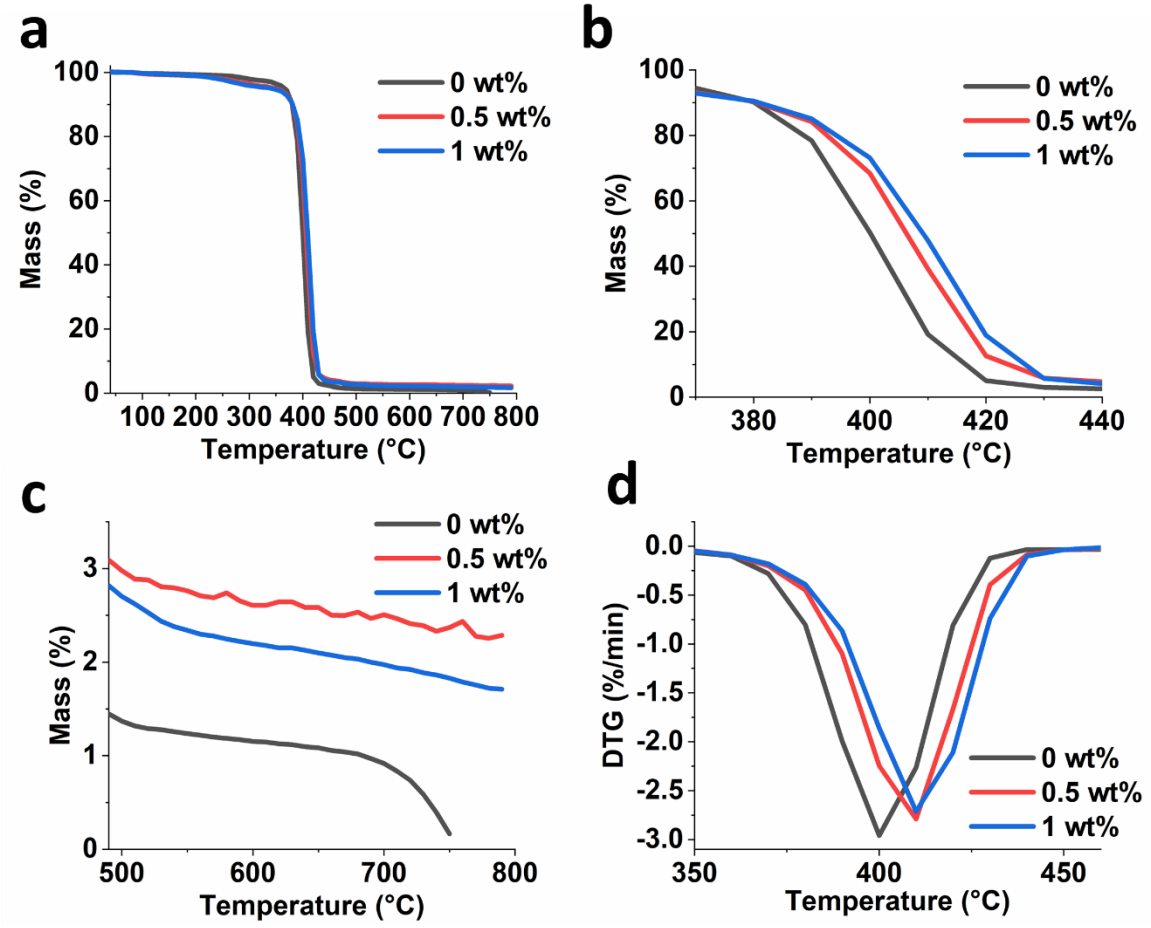

Fig. 5. (a) TGA curves, (b) enlarged temperature range 360 – 440 °C, (c) enlarged temperature range 500 – 800 °C, and (d) enlarged temperature range in DTG curves 350 – 450 °C for the neat polymer and composites

.

Table 6

Yield strength, modulus of elasticity, tensile strength, strain at break, and toughness for the neat polymer and the composite samples

Sample	Yield strength (MPa)	Young modulus (MPa)	Tensile strength (MPa)	Strain at break (%)	Toughness (MJ/m^3)
P(MMA/BA/AAm)	0.108 ± 0.007	12.725 ± 0.7	1.124 ± 0.05	369.43 ± 33.43	2.94 ± 0.12
0.5wt% L/P(MMA/BA/AAm)	0.119 ± 0.006	6.407 ± 1.65	1.083 ± 0.31	412.14 ± 135.76	2.89 ± 1.24
1wt% L/P(MMA/BA/AAm)	0.140 ± 0.065	8.950 ± 4.20	1.312 ± 0.56	541.83 ± 15.39	4.06 ± 1.33

In Figure 6, the stress–strain graphs of the neat polymer and the composites are shown. The tensile test revealed that lignin incorporation into the polymer matrix led to a decrease in the elastic modulus, while the strain at break was increased. Literature reports suggest that lignin can act as a plasticiser when introduced into polymer matrices, which may explain this behaviour.[54,55]

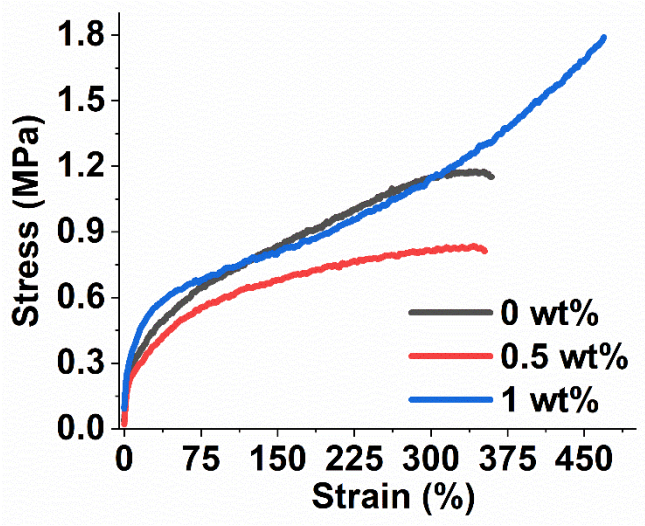

Fig. 6. Stress–strain graphs of the neat polymer and the composites

When comparing composites containing 0.5 wt% and 1 wt% lignin, the sample with 1 wt% lignin showed improved mechanical properties. This improvement was likely due to the higher lignin content and the resulting structural characteristics. As shown in Figures 4d–4f, the composite with 0.5 wt% lignin displayed pores in its cross-section, which acted as structural defects and impaired mechanical performance by hindering efficient stress transfer from the polymer matrix to the filler. This morphological feature likely explained the larger variability observed in strain at break values (Table 6) for this sample. In contrast, the 1 wt% lignin composite exhibited a more uniform and less porous morphology, contributing to a 1.5-fold increase in strain at break compared to the neat polymer. Likewise, it showed approximately a 1.4-fold increase in toughness. Additionally, this composite showed higher tensile strength and yield strength, indicating its ability to withstand greater stress without permanent deformation. The effect that 1 wt% lignin had on the mechanical properties of the polymer matrix was likely due to a balance between the plasticisation effect, originating from the weakened intermolecular forces between polymer chains induced from the presence of lignin, and local reinforcement from lignin's rigid structure. Most likely, at low concentration (1 wt%), lignin may not fully disrupt the polymer network, resulting in stiffer segments.

These findings suggested that a higher lignin concentration enhanced stress distribution within the matrix, leading to improved mechanical performance compared to the composite with 0.5 wt% lignin.

To assess composite behaviour under UV irradiation, free-standing films of the neat polymer and composites underwent accelerated aging test under UV irradiation at 366 nm for 364 hours. The chemical changes induced by accelerated aging were monitored using FTIR spectra recorded before and after irradiation. The areas of the hydroxyl group (3700–3060 cm^{-1}) and the ether group (1333–1075 cm^{-1}), as well as the peak height of the carbonyl functional group (1730 cm^{-1}) were evaluated (Fig.7).

The incorporation of lignin into the polymer matrix accelerated the degradation process. Hu et al. reported a similar effect using 10 wt% lignin combined with 0.5 wt% photocatalytic ZnO to promote PMMA degradation and facilitate recyclability.[34]After 100 h of UV irradiation, a 16% decrease in β-O-4 linkage frequency was observed for the lignin–PMMA composite and around 72% for the lignin–PMMA–ZnO system. In the present study, degradation was attributed solely to lignin, as no additional agents were employed. This behaviour was primarily due to lignin's strong UV–visible light absorption, arising from its aromatic structure and diverse chromophoric groups. UV absorption by lignin initiated key photochemical reactions, including dehydrogenation, dehydroxymethylation, and demethoxylation, as previ-

ously reported.[56] The commonly accepted mechanism for lignin photo-oxidation begins with free radical formation through the oxidation of phenolic hydroxyl groups. These phenolic radicals formed almost immediately under UV irradiation and subsequently promoted ortho- and para-quinone development after demethylation and side-chain cleavage.[56] An alternative degradation pathway involved UV-induced cleavage of ether linkages in lignin, resulting in depolymerisation and formation of various degradation products and free radicals, such as coniferyl alcohol and guaiacyl radicals. These species could undergo further reactions or trigger deeper degradation processes.[34,57]

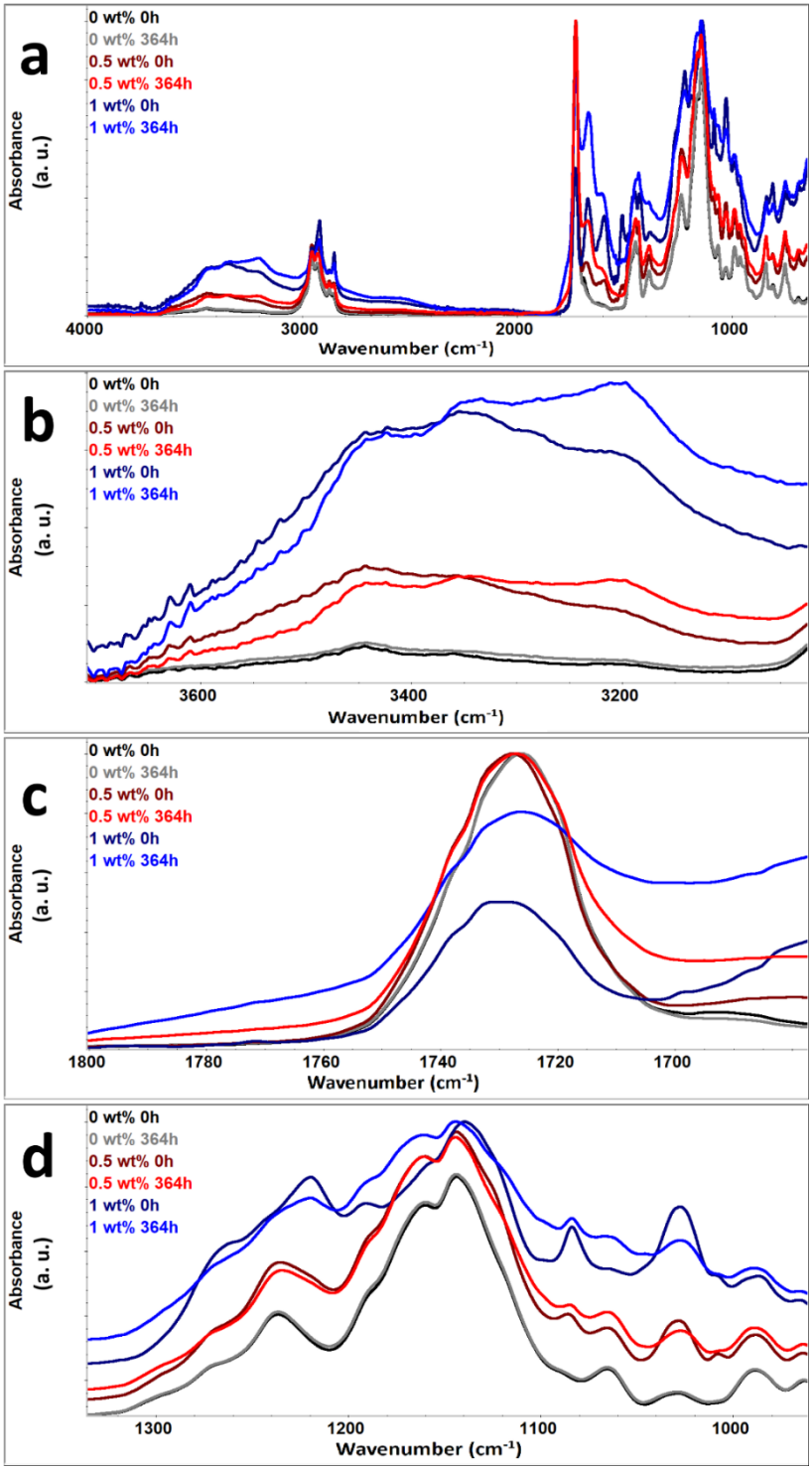

Fig. 7. FTIR spectra of the neat polymer and the different composites after 364 hours of irradiation at 366 nm: (a) overall spectra, (b) –OH stretching region (3700 – 3100 cm^{-1}), (c) C=O stretching region (1850 – 1550 cm^{-1}), and (d) C–O–C stretching region (1333 – 1075 cm^{-1})

In Figure 8, the areas and the peak height of the examined characteristic bands are presented. Figure 8 indicated that both the neat polymer and the composite underwent structural changes as a result of ageing, with these changes being more pronounced in the composites. Photo-oxidative degradation of acrylate polymers typically involved polymer chain scission, elimination of side groups, and breakdown of lateral chains.[39] Specifically, the degradation pathway involved the removal of ester side chains, leading to changes in the area and intensity of characteristic infrared bands associated with hydroxyl, ether, and carbonyl functional groups. The observed decreases in the ether and carbonyl bands supported the conclusion that degradation primarily occurred through the destruction of ester side chains in the polymer matrix. When comparing the neat polymer and the composites, it was evident that degradation was more severe in the presence of lignin, as the changes in the characteristic bands were lower in the neat polymer. For the hydroxyl band, a decrease was observed in the neat polymer, likely indicating the formation of low molecular weight volatile products or the occurrence of secondary reactions.[58] In contrast, the hydroxyl band in the composites showed a slight increase, which suggested the formation of new hydroxyl or hydroperoxide groups.

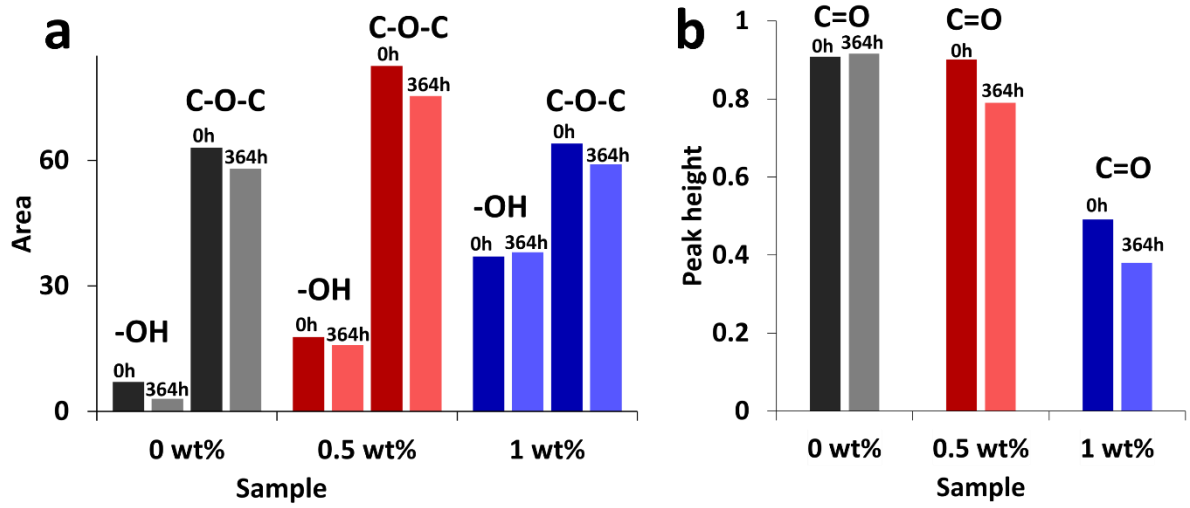

Fig. 8. (a) Areas below the –OH and C–O–C peaks and (b) height of the C=O peak in FTIR spectra of the neat polymer and composites containing 0.5 wt% and 1 wt% lignin

The UV-ageing behaviour of composites containing 0.5 wt% and 1 wt% lignin was compared. The results (Fig. 8) indicated no statistically significant difference in the degradation rate or extent between the two concentrations, which suggested that the radical scavenging and degradation-promoting effects of lignin were already near-maximised at 0.5 wt% in this system. The enhanced degradation observed in the lignin-containing composites highlighted the potential for controlled, triggered degradation, or depolymerisation of the material after its intended use.

The water resistance of materials determines the protective ability of the material and its durability. Figure 9 shows the water uptake by the polymer and the composite containing 1 wt% lignin when immersed in water during various time periods. Due to its poor mechanical properties, the sample with 0.5 wt% lignin was not investigated.

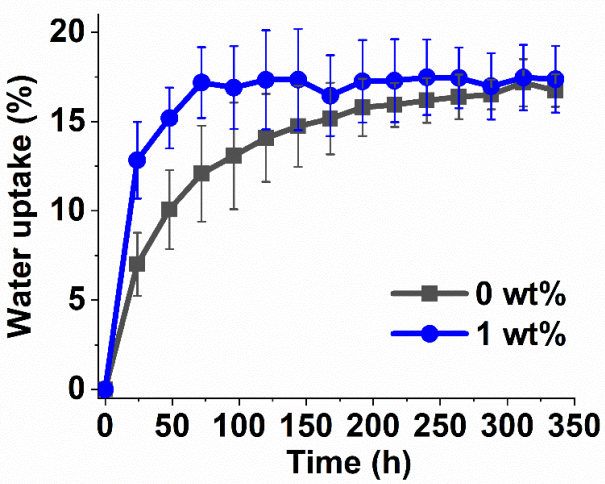

Fig. 9. Water uptake of the neat polymer and the 1 wt% lignin composite films as a function of immersion time in water

The presented data represented the mean of five measurements, with corresponding standard deviations also included. When comparing the composite containing 1 wt% lignin to the neat polymer, it was evident that during the initial phase of the test, particularly within the first 150 hours, the composite absorbed a higher percentage of water than the neat polymer. However, the composite reached saturation after just 72 hours, whereas the water absorption of the neat polymer continued to increase over time. The water uptake of the composite with 1 wt% lignin remained below 20 % over the entire measurement period of 350 h. For comparison, Messmer et al.[44] reported a water absorption of approximately 60 % for composites containing 1 wt% kraft lignin prepared via miniemulsion polymerisation, and about 23 % for those obtained by miniemulsion polymerisation after 110 h of measurement. The improved water absorption stability of the 1 wt% lignin composite was likely due to the uniform dispersion of lignin within the matrix, which acted as a physical barrier, limiting water penetration into the film.

Given that hydrolytic stability was a key property influencing the suitability of materials for various applications, the water diffusion coefficient was calculated for both the neat polymer and the composite with 1 wt% lignin. The diffusion coefficient (D) was calculated using Equation 4:

$$D = \frac{\pi h^2 (M_2 - M_1)^2}{16 M_m^2 \left(t_2^{1/2} - t_1^{1/2}\right)^2} \quad (4)$$

where h is the sample thickness, M_m is the percentage at maximum water absorption (calculated as the mean of two measurements, where no significant change was observed). Equation 5 represents the slope determined from the linear part of the curve M_t as a function of $t^{(1/2)}$, where t refers to time in seconds.[59]

$$\frac{(M_2 - M_1)^2}{\left(t_2^{1/2} - t_1^{1/2}\right)^2} \quad (5)$$

Figure 10 displays the M_t versus $t^{1/2}$ curves, along with the corresponding linear equations for both materials.

Table 7 shows the calculated water diffusion coefficients according to Equation4.The incorporation of lignin into the polymer matrix resulted in a 40 % reduction in the water diffusion coefficient compared to the neat polymer, which indicated a slower rate of water absorption. Similar results were reported for related systems.[55] This effect was in line with literature that demonstrated that lignin could serve as a molecular barrier to water transport by blocking hydrogen-bonding sites and forming hydrogen bonds that restricted water mobility,[27,60] as well as acting as a reinforcing agent that increased the complexity of the diffusion pathway and enhanced barrier properties.[61]The behaviour of the composite with 1 wt% lignin could further be explained by its complex internal structure, which was observed in the SEM micrographs (Figs. 4g–4i). Despite the surface hydrophilicity shown in Table 4, the intricate cross-sectional morphology provided an effective barrier to water penetration, thereby lowering the overall water uptake rate and improving the composite's stability.

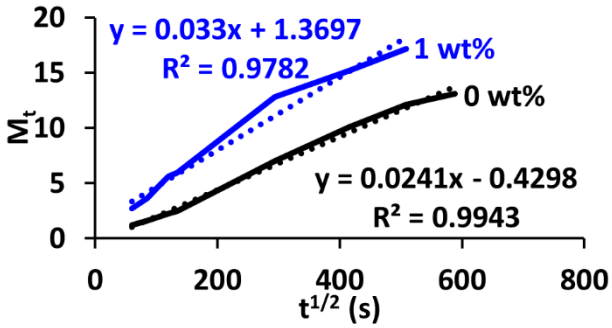

Fig. 10. M_t versus $t^{1/2}$ curves and the corresponding linear equations of the neat polymer and the composite containing 1 wt% lignin

T a b l e 7

Water diffusion coefficients of the neat polymer and the composite containing 1 wt% lignin

Sample	Water diffusion coefficient (m^2/s)
P(MMA/BA/AAm)	2.226×10^{-11}
1wt% L/P(MMA/BA/AAm)	1.375×10^{-11}

Overall, the addition of lignin improved both the mechanical and hydrolytic stability of the composites by reducing water absorption. However, it also accelerated the degradation of the polymer matrix under UV irradiation and ambient conditions. These combined properties suggested that (meth)acrylate/lignin composites hold promise for eco-friendly applications, such as biodegradable packaging materials or agricultural films designed for moisture retention, weed suppression, or temperature regulation.

4. CONCLUSION

Waterborne lignin-based polymer composites were synthesised via in situ miniemulsion polymerisation, with lignin gradually introduced into the monomer mixture throughout the polymer-

isation process. This strategy enhanced monomer conversion and yielded stable composites containing 0.5 wt% and 1 wt% lignin relative to the polymer. Infrared spectroscopy confirmed the successful incorporation of lignin into the polymer matrix.

The presence of lignin caused a red shift in the light absorption maximum of the composites, significantly increased their absorption in the visible region compared to the neat polymer.

Scanning electron microscopy revealed that incorporating 1 wt% lignin resulted in significant morphological changes in the composite compared to the neat polymer, with lignin appearing uniformly distributed throughout the matrix. At first glance, the presence of lignin appeared to increase the material's hydrophilicity, likely due to surfactant migration facilitated by lignin. However, after the surfactant was removed from the film surface, the composite exhibited increased hydrophobicity, comparable to that of the neat polymer. In addition to morphological effects, the introduction of small amounts of lignin improved the thermal stability of the composites, shifting the temperature corresponding to the maximum degradation rate to higher values relative to the neat polymer. Furthermore, incorporating 1 wt% lignin enhanced mechanical properties, including yield strength, tensile strength, toughness, and strain at break, when compared to the neat polymer.

Both the polymer and the composites containing 0.5 wt% and 1 wt% lignin were exposed to 366 nm UV radiation under ambient conditions for 364 hours, and the ageing process was monitored using infrared spectroscopy. The results revealed that the composite underwent more pronounced chemical changes upon UV exposure compared to the neat polymer. These findings suggested that the incorporation of lignin significantly enhanced the photo-oxidative degradation of the material, highlighting its potential for UV-triggered recyclability after use.

The hydrolytic stability of the materials was evaluated by immersing both the composites and the polymer in distilled water over time, tracking water absorption percentage, and calculating the water diffusion coefficient. Incorporation of 1 wt% lignin was found to reduce the rate of water uptake, with a 40 % decrease in the water diffusion coefficient compared to the neat polymer. This improvement was attributed to the barrier effect of lignin structures uniformly dispersed within the polymer matrix.

Lignin-based composites, with their modulated structure, tailored functionalities, and enhanced properties resulting from the presence of lignin, opened new avenues for the application of this class of materials.

Competing Interests. The authors declare that they have no competing interests.

Acknowledgements. The financial support of NATO Science for Peace Program (G6011) is gratefully acknowledged.

5. REFERENCES

(1) Kuan, H. T. N.; Tan, M. Y.; Shen, Y.; Yahya, M. Y. Mechanical properties of particulate organic natural filler-reinforced polymer composite: A review. *Composites and Advanced Materials* **2021**, *30*, 1–17. https://doi.org/10.1177/26349833211007502

(2) Ridho, M. R.; Agustiany, E. A.; Rahmi, D. n. M.; Madyaratri, E. W.; Ghozali, M.; Restu, W. K.; Falah, F.; Rahandi Lubis, M. A.; Syamani, F. A.; Nurhamiyah, Y.; Hidayati, S.; Sohail, A.; Karungamye, P.; Nawawi, D. S.; Iswanto, A. H.; Othman, N.; Mohamad Aini, N. A.; Hussin, M. H.; Sahakaro, K.; Hayeemasae, N.; Ali, M. Q.; Fatriasari, W. Lignin as green filler in polymer composites: development methods, characteristics, and potential applications. *Advances in Materials Science and Engineering* **2022**, *2022*, 1–33. https://doi.org/10.1155/2022/1363481

(3) Sztorch, B.; Brząkalski, D.; Pakuła, D.; Frydrych, M.; Špitalský, Z.; Przekop, R. E. Natural and synthetic polymer fillers for applications in 3D printing – FDM technology area. *Solids* **2022**, *3* (3), 508–548. https://doi.org/10.3390/solids3030034

(4) Ramesh, M.; Rajeshkumar, L.; Srinivasan, N.; Kumar, D.; Balaji, D. Influence of filler material on properties of fiber-reinforced polymer composites: A review. *e-Polymers* **2022**, *22*, 898–916. https://doi.org/10.1515/epoly-2022-0080.

(5) Gaspar, R.; Fardim, P. Lignin-based materials for emerging advanced applications. *Current Opinion in Green and Sustainable Chemistry* **2023**, *41*, 100834. https://doi.org/10.1016/j.cogsc.2023.100834.

(6) Fabbri, F.; Bischof, S.; Mayr, S.; Gritsch, S.; Jimenez Bartolome, M.; Schwaiger, N.; Guebitz, G. M.; Weiss, R. The biomodified lignin platform: A review. *Polymers* **2023**, *15* (17), 1694. https://doi.org/10.3390/polym15071694

(7) Horizon Databook. Lignin market size, share & trend analysis report by product (Lignosulfonates, Kraft lignin, organosolv lignin, others), by application, by region, and segment forecasts 2024–2030. Report ID: 978-1-68038-422-2.

(8) Liao, J. J.; Latif, N. H. A.; Trache, D.; Brosse, N.; Hussin, M. H. Current advancement on the isolation, characterization and application of lignin. *Int. J. Biol. Macromol*. **2020**, *162*, 985–1024. https://doi.org/10.1016/j.ijbiomac.2020.06.168

(9) Zhang, Y.; Naebe, M. Lignin: A review on structure, properties, and applications as a light-colored UV absorber. *ACS Sustainable Chem. Eng*. **2021**, *9* (4), 1427–1442. https://doi.org/10.1021/acssuschemeng.0c06998

(10) Sadeghifar, H.; Ragauskas, A. Lignin as a UV light blocker – A review. *Polymers* **2020**, *12* (5), 1134. https://doi.org/10.3390/polym12051134

(11) Jędrzejczak, P.; Collins, M. N.; Jesionowski, T.; Klapiszewski, L. The role of lignin and lignin-based materials in sustainable construction – A comprehensive review. *Int. J. Biol. Macromol*. **2021**, *187*, 624–650. https://doi.org/10.1016/j.ijbiomac.2021.07.125

(12) Gadioli, R.; Morais, J. A.; Waldman, W. R.; De Paoli, M.-A. The role of lignin in polypropylene composites

with semi-bleached cellulose fibers: Mechanical properties and its activity as antioxidant. *Polymer Degradation and Stability* **2014**, *108*, 23–34. https://doi.org/10.1016/j.polymdegradstab.2014.06.005.

(13) Gadioli, R.; Waldman, W. R.; De Paoli, M.-A. Lignin as a green primary antioxidant for polypropylene. *J. Appl. Polym. Sci*. **2016**, *133* (45), 43558. https://doi.org/10.1002/app.43558

(14) Avelino, F.; De Oliveira, D. R.; Mazzetto, S. E.; Lomonaco, D. Poly(methyl methacrylate) films reinforced with coconut shell lignin fractions to enhance their UV-blocking, antioxidant and thermo-mechanical properties. *Int. J. Biol. Macromol*. **2019**, *125*, 171–180. https://doi.org/10.1016/j.ijbiomac.2018.12.043

(15) Huang, W.; Wu, M.; Liu, W.; Hua, Z.; Wang, Z.; Zhou, L. Value-adding of organosolv lignin: Designing mechanically robust UV-resistant polymeric glass via AR-GET ATR. *Applied Surface Science* **2019**, *475*, 302–311. https://doi.org/10.1016/j.apsusc.2018.12.266

(16) Yang, W.; Rallini, M.; Wang, D.-Y.; Gao, D.; Dominici, F.; Torre, L.; Kenny, J. M.; Puglia, D. Role of lignin nanoparticles in UV resistance, thermal and mechanical performance of PMMA nanocomposites prepared by a combined free-radical graft polymerization/masterbatch procedure. *Composites*: Part A **2018**, *107*, 61–69. https://doi.org/10.1016/j.compositesa.2017.12.030

(17) Hararak, B.; Wanmolee, W.; Wijaranakul, P.; Prakymoramas, N.; Winotapun, C.; Kraithong, W.; Nakason, K. Physicochemical properties of lignin nanoparticles from softwood and their potential application in sustainable pre-harvest bagging as transparent UV-shielding films. *Int. J. Biol. Macromol*. **2023**, *229*, 575–588. https://doi.org/10.1016/j.ijbiomac.2022.12.270

(18) Xin, Q.; Li, H.; Sun, W.; Li, X.; Lu, X.; Zhao, J. Lignin-xylan nanospheres prepared by green and quick method from lignocellulose and used as additive in PVA films. *Int. J. Biol. Macromol*. **2024**, *264*, 129762. https://doi.org/10.1016/j.ijbiomac.2024.129762

(19) Fan, D.; Chen, J.; Kong, M.; Lv, Y.; Huang, Y.; Li, G. Valorization of enzymatic hydrolysis lignin for the multifunctional stabilization of polypropylene. *Ind. Crops Prod*. **2022**, *187*, 115443. https://doi.org/10.1016/j.indcrop.2022.115443

(20) Yang, H.; Yu, B.; Xu, H.; Bourbigot, S.; Wang, H.; Song, P. Lignin-derived bio-based flame retardants toward high-performance sustainable polymeric materials. *Green Chem*. **2020**, *22* (7), 2129–2161. https://doi.org/10.1039/D0GC00449A

(21) Mandlekar, N.; Cayla, A.; Rault, F.; Giraud, S.; Salaün, F.; Malucelli, G.; Guan, J.-P. An overview on the use of lignin and its derivatives in fire retardant polymer systems. In: M. Poletto (Ed.), *Lignin – Trends and Applications*, InTech. **2018**. Available at: http://dx.doi.org/10.5772/intechopen.72963

(22) Chollet, B.; Lopez-Cuesta, J.-M.; Laoutid, F.; Ferry, L. Lignin nanoparticles as a promising way for enhancing lignin flame retardant effect in polylactide. *Materials* **2019**, *12* (13), 2132. https://doi.org/10.3390/ma12132132

(23) Zhang, S.; Meng, X.; Bhagia, S.; Ji, A.; Dean Smith, M.; Wang, Y.-Y.; Liu, B.; Yoo, C. G.; Harper, D. P.; Ragauskas, A. J. 3D printed lignin/polymer composite with enhanced mechanical and anti-thermal-aging performance. *Chem. Eng. J.* **2024**, *481*, 148449. https://doi.org/10.1016/j.cej.2023.148449

(24) Podkościelna, B.; Wnuczek, K.; Goliszek, M.; Klepka, T.; Dziuba, K. Flammability tests and investigations of properties of lignin-containing polymer composites based on acrylates. *Molecules* **2020,** *25* (24), 5947. https://doi.org/10.3390/molecules25245947

(25) Klapiszewski, L.; Podkościelna, B.; Goliszek, M.; Kubiak, A.; Młynarczyk, K.; Jesionowski, T. Synthesis, characterization and aging tests of functional rigid polymeric biocomposites with kraft lignin. *Int. J. Biol. Macromol*. **2021**, *178*, 344–353. https://doi.org/10.1016/j.ijbiomac.2021.02.193

(26) Domínguez-Robles, J.; Larrañeta, E.; Fong, M. L.; Martin, N. K.; Irwin, N. J.; Mutjé, P.; Tarrés, Q.; Delgado-Aguilar, M. Lignin/poly(butylene succinate) composites with antioxidant and antibacterial properties for potential biomedical applications. *Int. J. Biol. Macromol*. **2020**, *145*, 92–99. https://doi.org/10.1016/j.ijbiomac.2019.12.146

(27) Buzarovska, A.; Blazevska-Gilev, J.; Perez-Martnez, B. T.; Balahura, L. R.; GradisteanuPircalabioru, G.; Dinescu, S.; Costache, M. Poly(l-lactic acid)/alkali lignin composites: properties, biocompatibility, cytotoxicity and antimicrobial behavior. *J. Mater. Sci*. **2021**, *56*, 13785–13800. https://doi.org/10.1007/s10853-021-06185-6

(28) Xu, C.; Liu, L.; Renneckar, S.; Jiang, F. Chemically and physically crosslinked lignin hydrogels with antifouling and antimicrobial properties. *Ind. Crops Prod*. **2021**, *170*, 113759. https://doi.org/10.1016/j.indcrop.2021.113759

(29) Jiang, C.; Wang, X.; Qin, D.; Da, W.; Hou, B.; Hao, C.; Wu, J. Construction of magnetic lignin-based adsorbent and its adsorption properties for dyes. *J. Hazard. Mater.* **2019**, *369*, 50–61. https://doi.org/10.1016/j.jhazmat.2019.02.021

(30) Şimşek, S. Adsorption properties of lignin containing bentonite–polyacrylamide composite for ions. *Desalination and Water Treatment* **2016,** *57* (50), 23790–23799. https://doi.org/10.1080/19443994.2015.1135478

(31) Meng, X.; Scheidemantle, B.; Li, M.; Wang, Y.; Zhao, X.; Toro-González, M.; Singh, P.; Pu, Y.; Wyman, C. E.; Ozcan, S.; Cai, C. M.; Ragauskas, A. J. Synthesis, characterization, and utilization of a lignin-based adsorbent for effective removal of azo dye from aqueous solution. ACS omega **2020**, *5* (6), 2865–2877. https://doi.org/10.1021/acsomega.9b03717

(32) Kayan, G. O.; Kayan, A. Composite of natural polymers and their adsorbent properties on the dyes and heavy metal ions. *J. Polym. Environ*. **2021**, *39*, 3477–3496. http://dx.doi.org/10.1007/s10924-021-02154-x

(33) Aldajani, M.; Alipoormazandarani, N.; Kong, F.; Fatehi, P. Acid hydrolysis of kraft lignin-acrylamide polymer to improve its flocculation affinity. *Sep. Purif. Technol*. **2021**, *258*, 117964. http://dx.doi.org/10.1016/j.seppur.2020.117964.

(34) Hu, C.; Zhao, M.; Li, Q.; Liu, Z.; Hao, N.; Meng, X.; Li, J.; Lin, F.; Li, C.; Fang, L.; Dai, S. Y.; Ragauskas, A. J.; Sue, H. J.; Yuan, J. S. Phototunable lignin plastics to enable recyclability. *ChemSusChem* **2021**, *14* (19), 4260–4269. https://doi.org/10.1002/cssc.202101040

(35) Chaochanchaikul, K.; Jayaraman, K.; Rosarpitak, V.; Sombatsompop, N. Influence of lignin content on photodegradation in wood/HDPE composites under UV weathering. *BioResources* **2012**, *7* (1), 38–55. http://dx.doi.org/10.15376/biores.7.1.38-55

(36) Goliszek, M.; Podkościelna, B.; Sevastyanova, O.; Fila, K.; Chabros, A.; Pączkowski, P. Investigation of accelerated aging of lignin-containing polymer materials. *Int. J. Biol. Macromol*. **2019**, *123*, 910–922. https://doi.org/10.1016/j.ijbiomac.2018.11.141

(37) Tang, Y.; Ye, Z.; Jean, M. Influence of lignin accessibility on chemical and biological decomposition of lignin/polyethylene composite thermoplastics. *Can. J. Chem. Eng*. **2020**, *98* (1), 104–118. https://doi.org/10.1002/cjce.23623

(38) Prosheva, M.; Ehsani, M.; Joseph, Y.; Tomovska, R.; Blazhevska Gilev, J. Waterborne polymer composites containing hybrid graphene/carbon nanotube filler: Effect of graphene type on properties and performance. *Polymer Composites* **2023**, *44* (8), 5188–5200. https://doi.org/10.1002/pc.27483

(39) Prosheva, M.; Aboudzadeh, M. A.; Leal, G. P.; Blazevska Gilev, J.; Tomovska, R. High-performance UV protective waterborne polymer coatings based on hybrid graphene/carbon nanotube radicals scavenging filler. *Part. Part. Syst. Charact*. **2019**, *36* (7), 1800555. https://doi.org/10.1002/ppsc.201800555

(40) Moreno, A.; Morsali, M.; Liu, J.; Sipponen, M. H. Access to tough and transparent nanocomposites via Pickering emulsion polymerization using biocatalytic hybrid lignin nanoparticles as functional surfactants. *Green Chem*. **2021**, *23* (8), 3001–3014. https://doi.org/10.1039/D1GC00103E

(41) Faucheu, J.; Gauthier, C.; Chazeau, L.; Cavaillé, J.; Mellon, V.; Lami, E. B. Miniemulsion polymerization for synthesis of structured clay/polymer nanocomposites: Short review and recent advances. *Polymer* **2009**, *51* (1), 6–17. https://doi.org/10.1016/j.polymer.2009.11.044

(42) El-Aasser, M. S.; Sudol, E. D. Miniemulsions: overview of research and applications. *JCT Research* **2004**, *1* (1), 20–31.

(43) Assumpção, N. R. L.; Lona, L. M. F. Effect of lignin without surface treatment in in situ methyl methacrylate miniemulsion polymerization. *ACS Sustainable Chem. Eng.* **2022**, *10* (10), 3219–3226. https://doi.org/10.1021/acssuschemeng.1c07467

(44) Messmer, N. R.; Guerrini, L. M.; Oliveira, M. P. Effect of unmodified kraft lignin concentration on the emulsion and miniemulsion copolymerization of styrene with n-butyl acrylate and methacrylic acid to produce polymer hybrid latex. *Polym. Adv. Technol*. **2018**, *29* (3), 1094–1106. https://doi.org/10.1002/pat.4221

(45) Prosheva, M.; Ozmen-Monkul, B.; Gumus, G.; Taskin, D. K.; Trajcheva, A.; Blazevska-Gilev, J.; Tomovska, R. Waterborne advanced optical coatings based on polymer composite with hybrid graphene-metal phthalocyanine nanofiller. *Prog. Org. Coat.* **2025**, *204,* 109260. https://doi.org/10.1016/j.porgcoat.2025.109260

(46) Owens, D. K.; Wendt, R. C. Estimation of the surface free energy of polymers. *Journal of Applied Polymer Science* **1969**, 13, 1741-1747. https://doi.org/10.1002/app.1969.070130815

(47) Argaiz, M.; Aguirre, M.; Tomovska, R. Strategies towards improved performance of waterborne coatings through multiplying the ionic interparticle interactions. *Prog. Org. Coat*. **2023**, *183*, 107731. https://doi.org/10.1016/j.porgcoat.2023.107731

(48) Chen, K.; Dong, W.; Huang, Y.; Wang, F.; Zhou, J. L.; Li, W. Photocatalysis for sustainable energy and environmental protection: A review on advanced surface engineering strategies and emerging synthesis methods. *J. Environ. Chem. Eng*. **2025**, *13*, 117529. https://doi.org/10.1016/j.jece.2025.117529

(49) Rozman, H.; Tan, K.; Kumar, R.; Abubakar, A.; Ishak, Z. M.; Ismail, H. The effect of lignin as a compatibilizer on the physical properties of coconut fiber–polypropylene composites. *Eur. Polym. J*. **2000**, *36* (7), 1483–1494. https://doi.org/10.1016/s0014-3057(99)00200-1

(50) Sameni, J.; Jaffer, S. A.; Sain, M. Thermal and mechanical properties of soda lignin/HDPE blends. *Compos.* Part A: *Appl. Sci. Manuf*. **2018**, *115*, 104–111. https://doi.org/10.1016/j.compositesa.2018.09.016

(51) Thielemans, W.; Wool, R. P. Butyrated kraft lignin as compatibilizing agent for natural fiber reinforced thermoset composites. *Compos*. Part A: *Appl. Sci. Manuf*. **2004**, *35* (3), 327–338. https://doi.org/10.1016/j.compositesa.2003.09.011

(52) Bilgina, S.; Tomovska, R.; Asua, J. M. Effect of ionic monomer concentration on latex and film properties for surfactant-free high solids content polymer dispersions. *Eur. Polym. J*. **2017**, *93*, 480–494. http://dx.doi.org/10.1016/j.eurpolymj.2017.06.029

(53) Mandlekar, N.; Cayla, A.; Rault, F.; Giraud, S.; Salaün, F.; Malucelli, G.; Guan, J. Thermal stability and fire retardant properties of polyamide 11 microcomposites containing different lignins. *Ind. Eng. Chem. Res*. **2017**, *56* (46), 13704–13714. https://doi.org/10.1021/acs.iecr.7b03085

(54) Soygun, K.; Şimşek, S.; Yılmaz, E.; Bolayır, G. Investigation of mechanical and structural properties of blend lignin-PMMA. *Adv. Mater. Sci. Eng*. **2013**, *2013*, 435260. http://dx.doi.org/10.1155/2013/435260

(55) Park, C.-W.; Youe, W.-J.; Kim, S.-J.; Han, S.-Y.; Park, J.-S.; Lee, E.-A.; Kwon, G.-J.; Kim, Y.-S.; Kim, N.-H.; Lee, S.-H. Effect of lignin plasticization on physicomechanical properties of lignin/poly(lactic acid) composites. *Polymers* **2019**, *11* (12), 2089. https://doi.org/10.3390/polym11122089

(56) Nikafshar, S.; Nejad, M. Evaluating efficacy of different UV-stabilizers/absorbers in reducing UV-degradation of lignin. *Holzforschung* **2022**, *76* (3), 235–244. https://doi.org/10.1515/hf-2021-0147

(57) Cogulet, A.; Blanchet, P.; Landry, V. Wood degradation under UV irradiation: A lignin characterization. *J. Photochem. Photobiol*. B **2016,***158*, 184–191. https://doi.org/10.1016/j.jphotobiol.2016.02.030

(58) Kaczmarek, H.; Kamińska, A.; Van Herk, A. Photooxidative degradation of poly(alkyl methacrylate)s. *Eur. Polym. J.* **2000**, *36* (4), 767–777. https://doi.org/10.1016/S0014-3057(99)00125-1.

(59) Tham, W. L.; Poh, B. T.; Mohd Ishak, Z. A.; Chow, W. S. Characterisation of water absorption of biodegradable poly(lactic acid)/halloysite nanotube nanocomposites at different temperatures. *J. Eng. Sci.* **2016**, *12*, 13–25.

(60) Vu, T.; Chaffee, A.; Yarovsky, I. Investigation of lignin-water interactions by molecular simulation. *Mol. Simul*. **2002,** *28* (10–11), 981–991. https://doi.org/10.1080/089270204000002610

(61) Shankar, S.; Reddy, J. P.; Rhim, J. Effect of lignin on water vapor barrier, mechanical, and structural properties of agar/lignin composite films. *Int. J. Biol. Macromol*. **2015**, *81*, 267–273. https://doi.org/10.1016/j.ijbiomac.2015.08.015